PROCEEDINGS OF SCIENCE

Identifying and Characterizing Air Shower Events with the Payload for Ultrahigh Energy Observations (PUEO)

Kaeli Hughes[a,*] **for the PUEO collaboration**

[a] *Pennsylvania State University,*
State College, PA, USA

E-mail: kaeli@psu.edu

The Payload for Ultrahigh Energy Observations (PUEO) is a balloon-borne neutrino observatory currently under construction and slated to fly in December 2025. PUEO will be sensitive to both Askaryan radio emission from neutrino interactions in the ice, and geomagnetic and Askaryan emission created from either cosmic ray interactions or tau leptons decaying. Separating the air shower emission from the Askaryan emission is critical to achieving PUEO's main science goal of measuring the flux of neutrinos above 1 EeV. In this contribution, I will describe how the sensitivity of PUEO's air shower channel has been improved relative to its predecessor, ANITA. In particular, in addition to the classic main instrument which targets emission in the 300-1200 MHz range, PUEO is deploying a drop-down low frequency (LF) instrument capable of independently triggering on air shower events with frequencies between 50-300 MHz. Together, the main instrument and the LF instrument will increase the number of air shower events detected by PUEO, measure the frequency content, polarity, and pointing resolution of candidate events, and will further investigate the origin of the anomalous ANITA events.

38th International Cosmic Ray Conference (ICRC2023)
26 July - 3 August, 2023
Nagoya, Japan

*Speaker

PoS(ICRC2023)1027

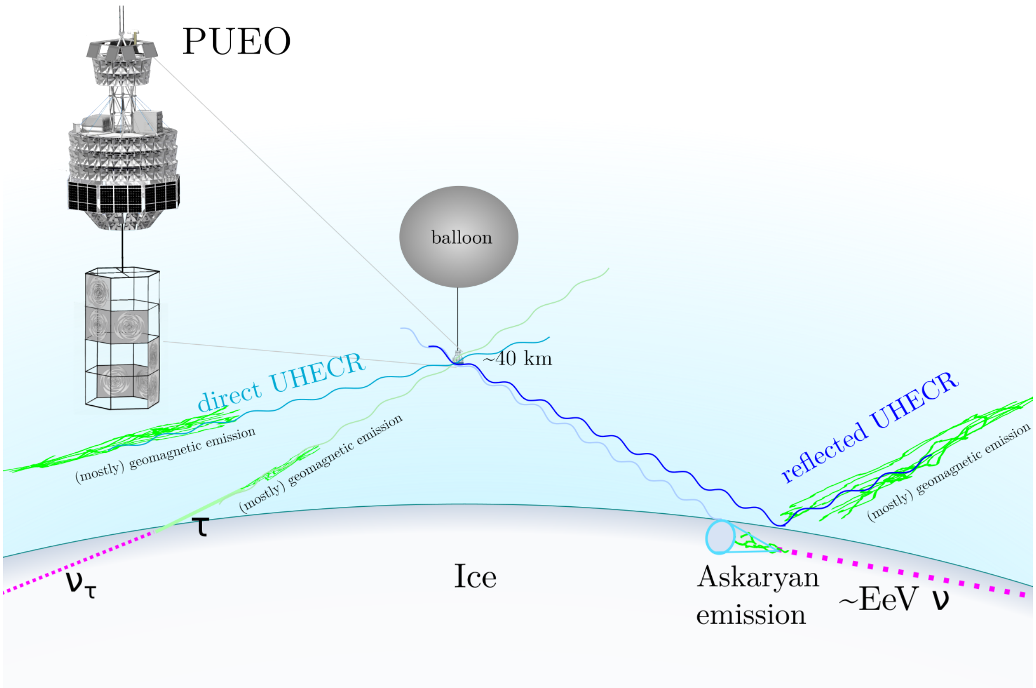

Figure 1: A diagram of the PUEO instrument and the types of radio emission from particles it will be capable of detecting. The direction, frequency content, polarity and polarization of the pulses differentiate the types of pulses.

1. Introduction

The Payload for Ultrahigh Energy Observations (PUEO) is a neutrino observatory currently under construction to fly around Antarctica in December 2025. PUEO is sensitive to the Askaryan radio emission that occurs when an ultra high energy (UHE) neutrino (above 10 PeV) interacts in the Antarctic ice [1, 4]. This radio emission is broadband and linearly polarized, and the long attenuation length for radio in Antarctic ice provides a natural detector medium for observing these rare events. PUEO will fly about 40 km above the continent and observe approximately 1.5 million square kilometers of ice. The large distance between the PUEO instrument and the potential interaction point of the neutrino makes PUEO especially suited for neutrinos above 10^{18} eV.

PUEO takes significant heritage from the ANITA flights, which successfully flew four times and has set world-leading limits on the diffuse neutrino flux above 10^{20} eV [5, 6, 12, 14]. The PUEO main instrument is designed to achieve greater sensitivity to the diffuse neutrino flux in one flight than all four ANITA flights combined; this is possible due to a beamforming trigger and a larger number of higher gain antennas [15]. The PUEO main instrument targets the 300-1200 MHz band.

While the PUEO main instrument is optimized to detect UHE neutrinos via the Askaryan effect, it is also sensitive to radio emission from ultra high energy cosmic ray (UHECR) events, which occur when charged particles interact in the atmosphere and create broadband geomagnetic radiation [3, 8]. Radio emission of air showers has been identified by many experiments, including previous flights of ANITA [7, 9]. PUEO is able to see these events both directly and reflected off the ice, as shown in Figure 1. Additionally, charged current ν_τ interactions can also induce air showers

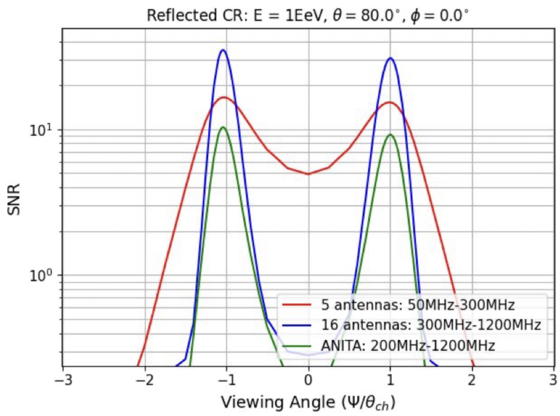

(a) SNR vs. Viewing Angle

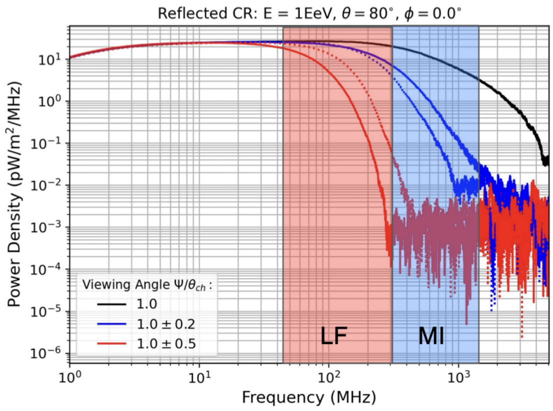

(b) Power density vs. Frequency

Figure 2: Left: The SNR of a simulated reflected cosmic ray event as a function of viewing angle (relative to the Cherenkov angle $\theta_{ch} \sim 0.6°$) for different frequency bands. Right: the power spectral density of a simulated reflected cosmic ray event. Targeting the lowest frequency range of 50-300 MHz will have the best chance of seeing a reflected cosmic ray event as the SNR is high across a large range of view angles.

when the resulting tau lepton decays [2]. These four types of signals (direct Askaryan, direct ν_τ shower, direct UHECR, and reflected UHECR) all differ with respect to their polarity, frequency content, and polarization. These metrics allow for separation at the analysis stage.

To better detect and identify air shower events, the PUEO payload will also fly a low-frequency (LF) instrument, which will target frequencies in the 50-300 MHz range. This drop-down array of eight dual-polarized canvas antennas will have its own trigger and will serve as an additional measurement of frequency content, polarity, and polarization.

In this work, we will discuss the motivation and design of the LF instrument, how it complements the main instrument, and the current status of simulation studies that are modeling PUEO's air shower channel. An overview of the PUEO Askaryan channel can be found in contribution [17].

2. Motivation from ANITA

As a neutrino detector, PUEO is primarily designed to detect both Askaryan emission from neutrino interactions, and geomagnetic and Askaryan emission from ν_τ and cosmic ray induced air showers. Over the course of four flights, in addition to setting limits on the diffuse neutrino flux, ANITA has detected 71 UHECR candidate events on a combined background of order 1. Seven are categorized as direct UHECR events, and 64 are categorized as reflected.

Additionally, three of the four ANITA flights have observed anomalous UHECR-like events, with directions consistent with reflected UHECRs but polarities consistent with direct UHECRs [10, 13]. Many hypotheses have been suggested for the origin of these events, including potential ν_τ-induced air showers. However, the steep direction of the events from ANITA-I and ANITA-III would not be consistent with limits set by other experiments for the current cross sections at these energies. ANITA-IV saw four upward showers, although unlike ANITA-I and ANITA-III, these events were all near the horizon and could more reasonably be explained by anthropogenic or

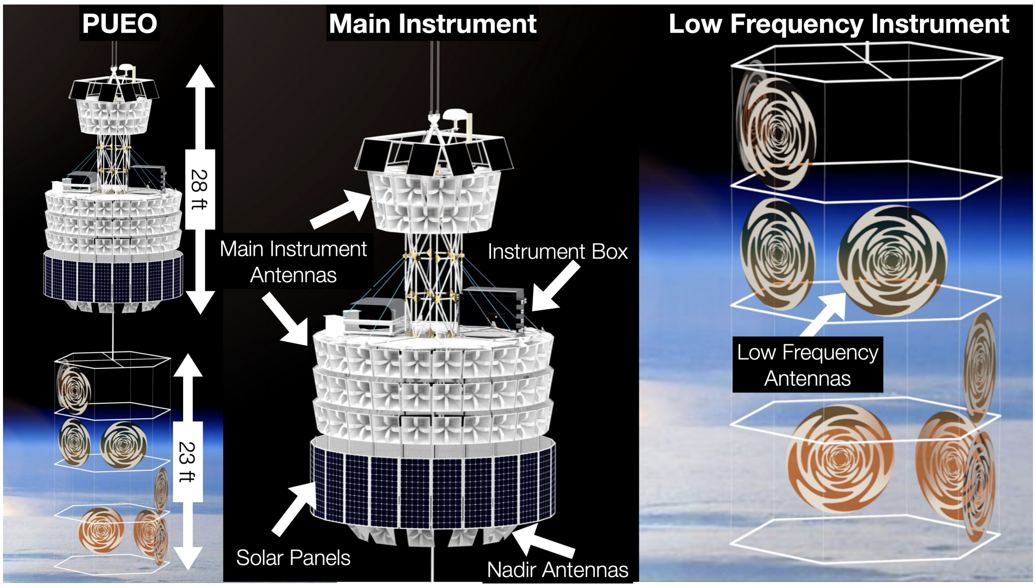

Figure 3: A diagram showing the PUEO instrument. Left panel: the full instrument as it will be deployed. Middle: the main instrument, including the instrument box and 108 broadband dual polarized antennas. Right panel: The Low Frequency instrument, with 8 dual-polarized broadband antennas.

misidentification. However, these events are not in tension with standard model cross sections if they are caused by ν_τ-induced air showers [16].

PUEO has been designed to answer some of these lingering questions about the air shower channel. Across the main and LF instruments, PUEO will span a broader frequency range than ANITA, and the additional low frequency sensitivity will help identify air shower events even for view angles that are far from the Cherenkov angle, as shown in Figure 2a and Figure 2b. PUEO also boasts more channels than ANITA in the main instrument, which will result in better pointing and thus better categorization of upward- and downward-going air showers in the data set. Combined with the LF instrument, PUEO will record significantly more information about its triggered events than any of the previous ANITA missions.

3. The PUEO Instrument

3.1 The Main Instrument

The main instrument, shown in Figure 3, shares many aesthetic similarities with its predecessor ANITA. Consisting of five rings of broadband, quad-ridged horn antennas, PUEO is able to fit more antennas onto its payload because of their slightly smaller size compared to the ANITA horns. PUEO is also designed around a two-step, beamforming phased array trigger, in which signals from antennas in the neighboring phi-sectors are added and summed in pre-determined directions to maximize the sensitivity to even low-threshold impulsive events. An overview of the main instrument can be found in contribution [18].

The main instrument also includes 12 nadir antennas, also shown in Figure 3, deployed after launch to hang below the payload at an angle of $-30°$. These antennas provide a longer baseline for

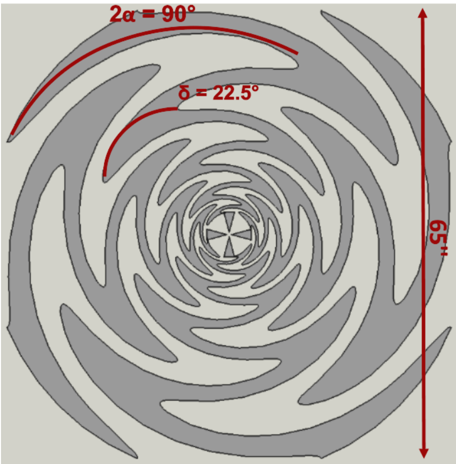

(a)

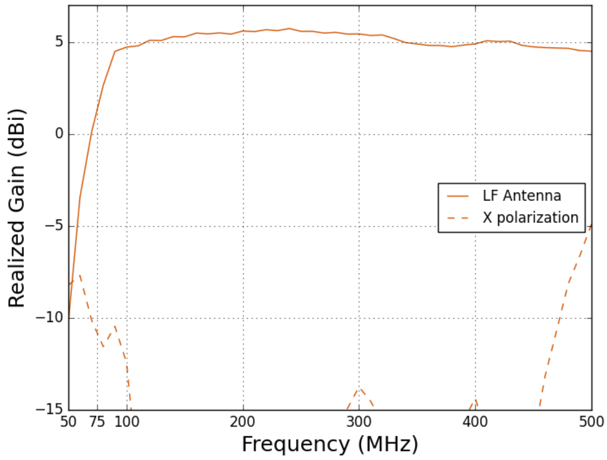

(b)

Figure 4: Left: A close up of the LF sinuous antenna. Right: a plot of the frequency response of the LF antenna. The response is fairly uniform across the 90-500 MHz band.

better reconstruction of events near the horizon, and their angled deployment gives PUEO increased sensitivity to backgrounds from the continent.

3.2 The Low Frequency Instrument

The LF antennas will be dual-polarized, broadband, and approximately 65" by 65" in size, designed to be easily stowed under the main instrument during launch. This stowed design is based on the ANITA-III low frequency antenna (ALFA) which was similarly deployed after launch. This allows the payload to fit within the dimension constraints set by the CSBF launch vehicle.

The LF instrument will be deployed in four vertical layers, with the antennas cascading downwards in a spiral pattern as shown in Figure 4a. The locations of the antennas have been optimized for the best coverage of all azimuthal directions and minimal interferance between adjacent antennas. Each antenna is a dual-polarized sinuous design, with both horizontally-polarized (HPol) and vertically-polarized (VPol) channels co-located on a single panel. The performance of these antennas, shown in Figure 4b, is fairly uniform across a broad range of frequencies. Because of this, we are considering extending the upper end of the LF instrument from 300 MHz to 500 MHz.

The LF antennas will be printed with conductive fabric, made with a Ni/Cu/Ag coating on Polymide/Nylon ripstop. This was selected for its resistivity and resilience to thermal cycling. The backing material is standard polyester often using in sailing applications and was selected due to its high UV resistance. To conduct tests of the stowing and deployment of the antennas, a half-sized model was fabricated and tested at Penn State University. Of particular interest is cable management both for the LF instrument structure as well as the cables to the antennas themselves. Cables will be folded in on themselves in the stowed configuration and auto-released via tension to their full lengths during the deployment. All parts for the LF instrument will be delivered by the end of this summer.

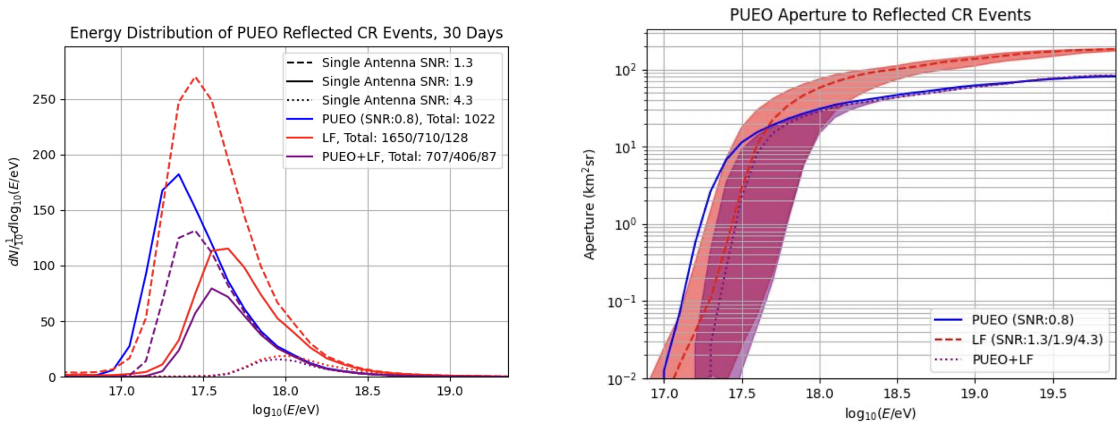

(a) Events vs. Energy.

(b) Aperture vs. Energy.

Figure 5: Left: the number of reflected cosmic ray events seen by each of PUEO's instruments as a function of primary energy. The different line styles are three possible thresholds for the LF instrument. Right: The aperture of the PUEO instruments as a function of reflected cosmic ray energy.

4. Simulation Studies

A variety of simulation tools have been developed to predict the PUEO instruments' sensitivity to air showers. These can be broken into three categories: (1) PUEOSim, a detector description that models both the main and LF instruments, (2) CRSim, to model the radio emission created by UHECR showers, and (3) TAPIOCA, to model the radio emission from ν_τ-induced air showers. The emission models and PUEOSim are directly integrated and designed to be modular, so that detector descriptions or emission models can be easily swapped in and out as needed. PUEO has a separate model for Askaryan emission called nicemc which is outside the scope of this proceedings.

As the LF instrument is still being designed, there is significant uncertainty in the expected threshold and trigger strategy. The threshold is determined by the noise rate, and current simulation studies suggest that a single antenna SNR threshold of 1.9σ is realistic. In addition to the realistic case, in the following plots, we show two other thresholds: an optimistic case with a threshold of 1.3σ; and a pessimistic case with a threshold of 4.3σ. The main PUEO instrument is expected to have a single antenna SNR threshold of 0.8σ. The LF instrument is currently modeled as a coherent sum trigger than uses five of the eight LF channels with the same polarization.

The results for reflected UHECR air showers is shown in Figure 5a and Figure 5b. In all cases, the LF instrument increases the number of UHECR events seen by PUEO, and this is especially true for energies above 10^{18} eV. At each potential trigger level, at least 40% of the events are seen by both the main instrument and the LF instrument. For these dual-triggered events, information about the frequency content, polarity, and polarization is expected to be quite robust. Additionally, because information is recorded from all antennas regardless of which instrument triggered, it is expected that additional information will be recovered from the LF instrument even when the event itself is below the LF trigger threshold. Work is ongoing to understand how this instrument will benefit at the analysis stage.

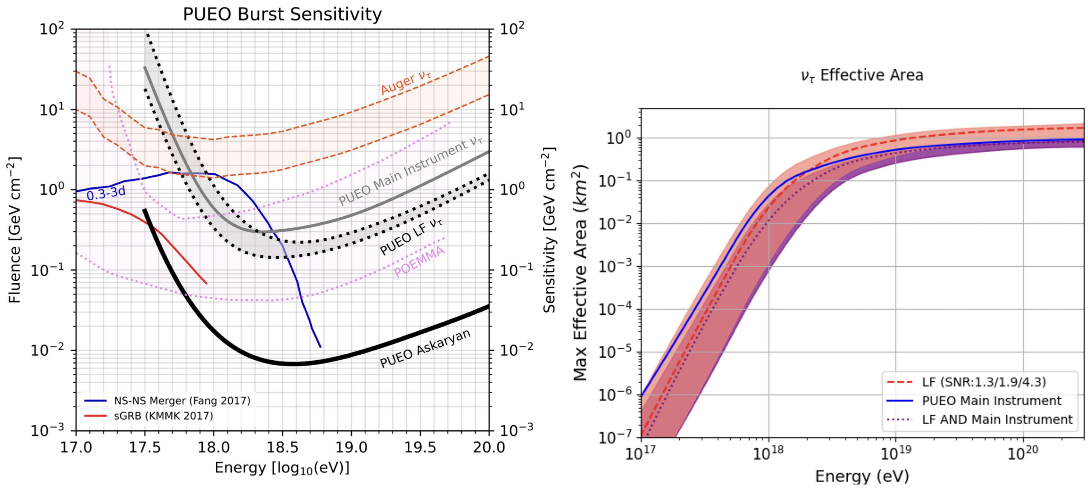

(a) Fluence vs. Energy.

(b) Effective Area vs. SNR.

Figure 6: Left: the fluence of the PUEO instrument in response to a burst event of length 0.3-3 days, compared to other experiments. Right: The ν_τ effective area as a function of ν_τ energy.

The results for the ν_τ-induced air showers are shown in Figure 6a and Figure 6b. While the Askaryan channel is expected to have significantly higher sensitivity than the air shower channel, the air shower channel is expected to have greater pointing resolution due to the small opening angle of the cone in air. Additionally, the air shower channel itself is expected to be sensitive enough to short burst events that it alone can detect or rule out certain models (e.g. [11]). Both the main instrument and the LF instrument are able to achieve this goal, but the LF instrument is more sensitive for showers with energies above 10^{18} eV.

Because PUEO will be capable of independently distinguishing ν_τ-induced air showers from the multi-flavor Askaryan channel, it could make simultaneous measurements of a single source in both channels. This is especially likely for a flaring source like those in Figure 6a. For events around 10^{18} eV, this could directly probe the ratio of ν_τ/ν_e events, as the Askaryan channel at these energies is expected to be dominated by ν_e interactions. This could provide specific insight into neutrino production mechanisms at these energies and could also provide a measurement of fundamental physics in a new energy regime.

5. Conclusion

The PUEO instrument will have significant sensitivity to air shower events. Current modeling suggests that PUEO will see O(1000) cosmic ray candidate events, an orders of magnitude increase compared to all four ANITA flights combined. This level of detection will lead to better characterization and identification of air shower events. These events are an important background to PUEO's main Askaryan channel, but could also lead to discoveries in the ν_τ-induced air shower category.

Early benchmarks for the expected performance of the LF instrument show that the instrument is expected to meet its performance goals. Future work will include modeling the reconstruction capability of the LF instrument, including direction, polarization, and polarity of incoming signals. PUEO is on track to be fully integrated well ahead of its December 2025 flight.

References

[1] G.A. Askaryan. "Excess negative charge of an electron-photon shower and its coherent radio emission". In: *Sov.Phys.JETP* (1961).

[2] Jonathan L. Feng et al. "Observability of Earth-Skimming Ultrahigh Energy Neutrinos". In: *Phys. Rev. Lett.* 88 (16 Apr. 2002), p. 161102. doi: 10.1103/PhysRevLett.88.161102.

[3] T. Huege and H. Falcke. "Radio emission from cosmic ray air showers: Simulation results and parametrization". In: *Astroparticle Physics* 24.1 (2005), pp. 116–136. issn: 0927-6505.

[4] The ANITA Collaboration. "Observations of the Askaryan Effect in Ice". In: *Phys.Rev.Lett.99* (2007).

[5] P. W. Gorham et. al. "The ANITA Ultra-high Energy Neutrino Detector Design, Performance, and Sensitivity for 2006-2007 Balloon Flight". In: *Astroparticle Physics* 32 (2009).

[6] P. W. Gorham et. al. "Observational Constraints on the Ultra-high Energy Cosmic Neutrino Flux from the Second Flight of the ANITA Experiment". In: *Phys. Rev. D.* 82 (2010).

[7] S. Hoover et al. "Observation of Ultrahigh-Energy Cosmic Rays with the ANITA Balloon-Borne Radio Interferometer". In: *Phys. Rev. Lett.* 105 (15 2010), p. 151101.

[8] J. Alvarez-Muñiz, W. R. Carvalho, and E. Zas. "Monte Carlo simulations of radio pulses in atmospheric showers using ZHAireS". In: *Astroparticle Physics* 35.6 (2012), pp. 325–341.

[9] A. Aab et al. "Measurement of the Radiation Energy in the Radio Signal of Extensive Air Showers as a Universal Estimator of Cosmic-Ray Energy". In: *Phys. Rev. Lett.* 116 (2016).

[10] P. W. Gorham et al. "Characteristics of Four Upward-Pointing Cosmic-Ray-like Events Observed with ANITA". In: *Phys. Rev. Lett.* 117 (7 Aug. 2016), p. 071101.

[11] K. Fang and B. Metzger. "High-energy Neutrinos from Millisecond Magnetars Formed from the Merger of Binary Neutron Stars". In: *The Astrophysical Journal* 849.2 (2017), p. 153.

[12] P. W. Gorham et. al. "Constraints on the diffuse high-energy neutrino flux from the third flight of ANITA". In: *Phys. Rev. D.* 98 (2018).

[13] P. W. Gorham et al. "Observation of an Unusual Upward-Going Cosmic-Ray-like Event in the Third Flight of ANITA". In: *Phys. Rev. Lett.* 121 (16 Oct. 2018), p. 161102.

[14] P.W. Gorham et. al. "Constraints on the ultra-high energy cosmic neutrino flux from the fourth flight of ANITA". In: *Phys. Rev. D.* 99 (2019).

[15] the ANITA Collaboration. "The Payload for Ultrahigh Energy Observations (PUEO): A White Paper". In: *submitted to JINST* (2020).

[16] R. Prechelt et al. "Analysis of a tau neutrino origin for the near-horizon air shower events observed by the fourth flight of ANITA". In: *Physical Review D* 105.4 (2022).

[17] C. Deaconu et. al. "Searching for Askaryan Emission from Neutrinos with the Payload for Ultrahigh Energy Observations (PUEO)". In: *Proceedings of Science, ICRC* (2023).

[18] Q. Abarr et. al. "Design of the next-generation ultrahigh energy neutrino observatory PUEO". In: *Proceedings of Science, ICRC* (2023).

Full Authors List: PUEO Collaboration

Q. Abarr[1], P. Allison[2], J. Alvarez-Muñiz[3], J. Ammerman Yebra[3], T. Anderson[4], A. Basharina-Freshville[5], J. J. Beatty[2], D. Z. Besson[6], R. Bose[7], D. Braun[7], P. Chen[8], Y. Chen[8], J. M. Clem[1], T. Coakley[2], A. Connolly[2], L. Cremonesi[9], A. Cummings[4], C. Deaconu[10], J. Flaherty[2], P. W. Gorham[11], C. Hornhuber[6], J. Hoffman[7], K. Hughes[4], A. Hynous[12], M. Jackson[2], A. Jung[11], Y. Ku[4], C.-Y. Kuo[8], G. Leone[10], C. Lin[1], P. Linton[2], T. C. Liu[13], W. Luszczak[2], S. Mackey[10], Z. Martin[10], K. McBride[2], C. Miki[11], M. Mishra[11], J. Nam[8], R. J. Nichol[5], A. Novikov[1], A. Nozdrina[6], E. Oberla[10], S. Prohira[6], R. Prechelt[11], H. Pumphrey[5], B. F. Rauch[7], R. Scrandis[10], D. Seckel[1], M. F. H. Seikh[6], J. Shiao[8], G. Simburger[7], G. S. Varner[11], A. G. Vieregg[10], S.-H. Wang[8], C. Welling[10], S. A. Wissel[4], C. Xie[5], R. Young[6], E. Zas[3], A. Zeolla[4]

[1]University of Delaware, [2]Ohio State University, [3]Universidade de Santiago de Compostela, [4]Pennsylvania State University, [5]University College London, [6]University of Kansas, [7]Washington University in St. Louis, [8]National Taiwan University, [9]Queen Mary University of London, [10]University of Chicago, [11]University of Hawaii, [12]NASA Wallops Flight Facility, [13]National Pingtung University